

Compact bandwidth-tunable microring resonators

Long Chen, Nicolás Sherwood-Droz, and Michal Lipson*

School of Electrical and Computer Engineering, Cornell University, Ithaca, New York 14853, USA

*Corresponding author: lipson@ece.cornell.edu

Received September 7, 2007; revised October 18, 2007; accepted October 24, 2007;
posted October 25, 2007 (Doc. ID 87295); published November 14, 2007

Using interferometric couplers and thermal tuning, we demonstrate a novel design of compact microring resonators on silicon-on-insulator platform with tunable bandwidth from 0.1 to 0.7 nm. The structures present an extinction ratio higher than 23 dB and a footprint of less than 0.001 mm², which are suitable for integrated optical signal processing such as reconfigurable filtering and routing. © 2007 Optical Society of America

OCIS codes: 130.3990, 130.7408.

Optical resonators can be used in a broad range of applications such as light generation, detection, and manipulation, including filtering, modulating, switching, etc. [1–6]. One key figure of merit of resonators is their bandwidth, i.e., the range in wavelength or frequency the resonances span, which is inversely proportional to the photon lifetime and quality factor (Q). While a narrow bandwidth (high Q) is suitable for enhancing light–matter interactions such as lasing [7] and sensing [8], a wide bandwidth (low Q), on the other hand, allows for optical signals of a broader spectrum and higher speed [9] and is more tolerant to variations in the environment.

Several applications require resonators with a tunable bandwidth or Q . One example is a reconfigurable channel selector for wavelength division multiplexing systems where the bandwidth of an add-drop filter can be tuned to accommodate one or several channels within one resonance and switch them simultaneously [10]. Here we demonstrate a compact microring resonator on silicon-on-insulator where the bandwidth can be continuously tuned from 0.1 to 0.7 nm with a 23 dB extinction ratio. We also show that, with improved coupling design and fabrication, this tuning range can be further expanded to from 0.01 to a few nanometers.

The bandwidth of a resonator is determined by its intrinsic loss and coupling with the input and/or output ports. Consider an add-drop microring as shown in Fig. 1(a). Assume that the round-trip intrinsic power loss is α ($\ll 1$) and that the power coupling with the input and output waveguides is κ and κ' , respectively. After each round trip the optical power circulating in the ring is reduced by a factor of $G \approx (1 - \alpha) \times (1 - \kappa)(1 - \kappa')$ [11]. The full width at half-maximum bandwidth can be thus written as $\Delta\lambda = (2\pi n_g L)^{-1} \lambda_0^2 \ln[1/G]$, where λ_0 and n_g are the resonant wavelength and group index, respectively, and $L = 2\pi R$ is the physical length of the ring. Any tuning of the loss or coupling results in a change in the bandwidth [12]. However, a high extinction ratio can only be obtained when “critical coupling” occurs, i.e., when $\kappa = \kappa' + \alpha$, in which case individual tuning leads to a degraded extinction ratio. Changing both κ and κ' accordingly so that $\kappa = \kappa' + \alpha$ remains valid enables

one to tune the bandwidth while maintaining a high extinction ratio.

The coupling of the resonator with the input and/or output ports can be changed dynamically with tunable interferometric couplers as shown in Fig. 1(b) [13,14]. Assume that the power coupling at each point is κ_0 and that the transmission and phase of the bus arm and ring arm are t_b, t_r (close to 1) and ϕ_b, ϕ_r , respectively. We can write the effective coupling from the waveguide to the ring as $\kappa = \kappa_0(1 - \kappa_0) \times (t_b + t_r - 2\sqrt{t_b t_r} \cos(\phi_b - \phi_r))$. As we change the relative phase $\Delta\phi = \phi_b - \phi_r$ from 0 to π (by means of thermo-optical, electro-optical, or all-optical effect), κ changes from 0 to $\sim 4\kappa_0(1 - \kappa_0)$. Figure 1(c) plots $\Delta\lambda$ against $\Delta\phi$ on a semilog scale for several values of κ_0 , using parameters typical of ring resonators in silicon [15,16]: $\lambda_0 = 1.55 \mu\text{m}$, $n_g = 4.2$, $R = 10 \mu\text{m}$, and an attenuation constant of 2.5 dB/cm ($\alpha = 0.004$, $t_b = 0.998$, $t_r = 0.999$). One can see the bandwidth can be tuned from 0.01 nm to a few nanometers.

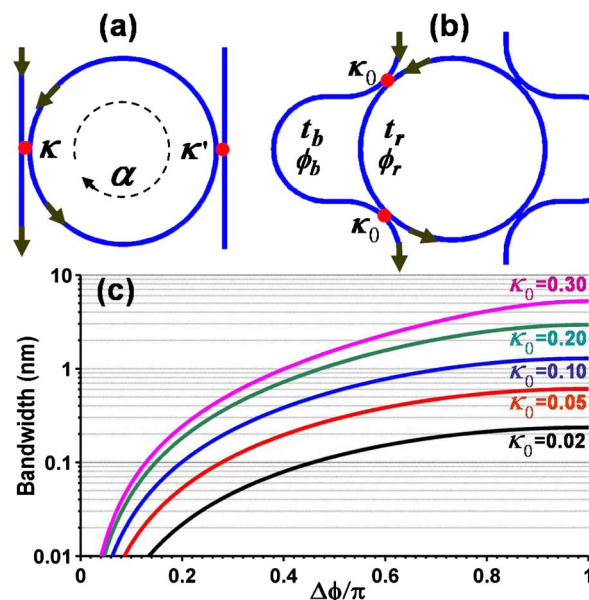


Fig. 1. (Color online) Schematics of an add-drop microring resonator with (a) straight couplers and (b) interferometric couplers. (c) Tuning of the bandwidth with $\Delta\phi$ under different coupling κ_0 .

We fabricate such bandwidth-tunable microring resonators using the thermo-optical effect as a tuning mechanism. Figures 2(a) and 2(b) show optical and scanning electron microscope images of the device, respectively. The device is fabricated on a silicon-on-insulator substrate with $3\ \mu\text{m}$ buried oxide and $240\ \text{nm}$ silicon. The waveguides and rings are first defined with electron beam lithography and reactive ion etching. A top SiO_2 cladding is then deposited via plasma-enhanced chemical vapor deposition and planarized with chemical mechanical polishing to a final thickness of $1\ \mu\text{m}$. Last, microheaters and electrical contact pads are sequentially patterned with lithography, evaporation, and lift-off processes. The microheaters and contact pads consist of $100\ \text{nm}$ thick Ni and $150\ \text{nm}$ thick Au, respectively, and the total resistance is $\sim 160\ \Omega$ at room temperature. The waveguide and ring are $520\ \text{nm}$ wide, with bending radii of 5.78 and $10\ \mu\text{m}$, respectively. These waveguide dimensions are slightly multimode at $\lambda = 1.55\ \mu\text{m}$, with the effective indices for the fundamental and higher order TE-like modes being 2.55 and 1.57 , respectively. Only the fundamental mode is excited. The gap between the waveguide and ring is $50\ \text{nm}$ to achieve strong coupling for the tightly confined mode. The power coupling coefficient κ_0 is calculated to be 5.3% at $\lambda = 1.55\ \mu\text{m}$, and this corresponds to a maximal bandwidth $\Delta\lambda$ of $0.65\ \text{nm}$. The whole device has a footprint of only $0.001\ \text{mm}^2$, which is 5 orders of magnitude smaller than a previous device on glass with similar functionality [10] and thus allows dense integration for on-chip optical signal processing. We analyzed the thermal isolation property of our device with FEMLAB simulations. With the silicon waveguide locally heated up to 100°C , the surrounding temperature drops to room temperature about $15\ \mu\text{m}$ away from the heating source. Even better thermal isolation can be achieved by etching deep trenches between the devices.

Figure 2(c) shows the through port transmission

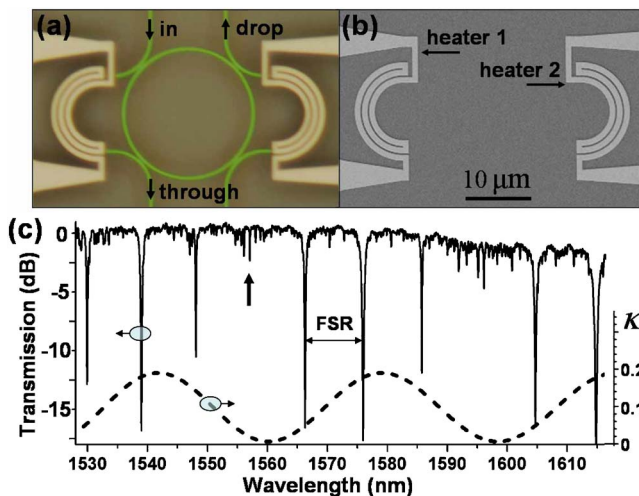


Fig. 2. (Color online) (a) Optical and (b) scanning electron microscope images of the device. (c) Measured through port transmission spectrum with both heaters off (solid curve). The effective coupling κ expected from theory is shown by the dashed curve.

for TE polarization normalized to reference waveguides. Multiple ring resonances are observed with a free spectral range of $\sim 9\ \text{nm}$. The resonances in this structure, contrary to resonances in standard ring resonators, exhibit distinctively different bandwidths and extinction ratios that are oscillating with wavelength. These oscillations originate from the wavelength dependence of κ since $\Delta\phi = 2\pi n_{\text{eff}}(L_b - L_r)/\lambda$, where n_{eff} is the effective index and L_b, L_r are the physical lengths of the two interfering arms. Taking $L_b - L_r = 15.68\ \mu\text{m}$ for this device, we sketch κ against λ in Fig. 2(c) as a dashed curve. Without any tuning $\kappa = \kappa'$ (symmetrical design), and therefore all resonances are initially “undercoupled” ($\kappa < \kappa' + \alpha$). The larger the κ , the broader the resonance and the closer it is to “critical coupling,” with a higher extinction ratio. Contrarily, with small κ , the resonance is severely “undercoupled” with a smaller extinction ratio. Similar oscillations in the bandwidths and extinction ratios are also observed in the drop port transmission. The insertion loss due to waveguide propagation is negligible for off-resonance wavelength considering the short length of the device.

Figure 3(a) shows the effect of tuning the input coupling κ with heater 1. The output coupling κ' is maintained constant. The device used here has $L_b - L_r = 15.53\ \mu\text{m}$, and the resonance measured is at $1586\ \text{nm}$. Starting from the “undercoupled” condition (I), the coupling first drops to a minimum (II) and then gradually moves across the “critical coupling” level (III) until the maximum (IV). Figure 3(b) shows the corresponding spectra, where the scale bar is $6\ \text{dB}$ for case (III) and $3\ \text{dB}$ for all others. One can see that the resonance can be completely switched off and on between state (II) and state (III). The resonant center wavelength changes slightly ($< 0.3\ \text{nm}$)

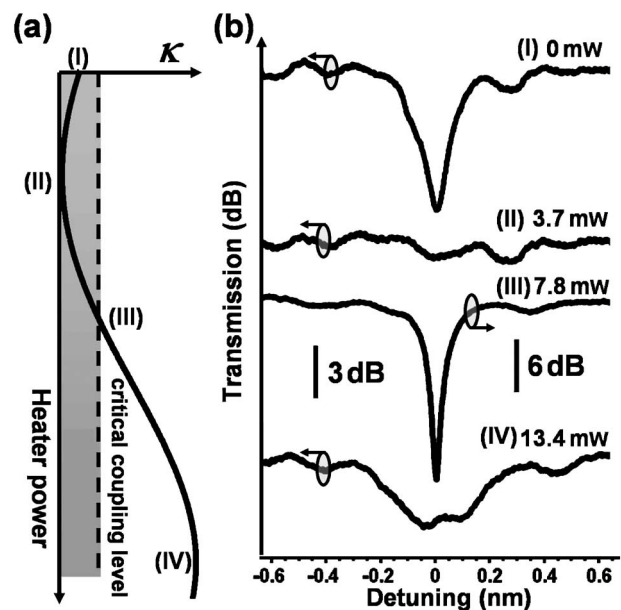


Fig. 3. (a) Tuning of κ with heater power: the dashed line marks the critical coupling level; (I), (II), (III), and (IV) mark the states of initial, minimal, critical, and maximal coupling, respectively. (b) Corresponding throughport spectra. Scale bar: $6\ \text{dB}$ for (III) and $3\ \text{dB}$ for the others.

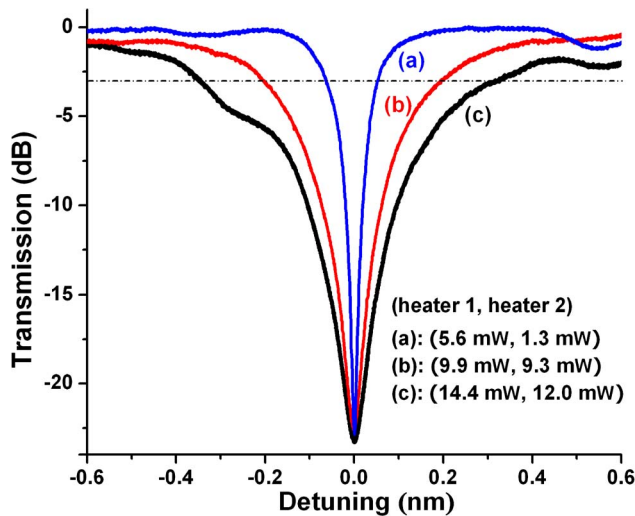


Fig. 4. (Color online) Tuning the bandwidth within “critical coupling” with both heaters. The dashed-dotted line marks the 3 dB level.

with increasing heater power, which can be stabilized with an additional heater on top of the ring, offsetting the ring temperature by ~ 3 °C. The fine structures mostly noticeable in (II) are Fabry–Perot oscillations caused by stitching points on the waveguide.

Tuning both coupling coefficients enables one to vary only the bandwidth while maintaining a high extinction ratio. Figure 4 shows the spectra under different heater powers for the same device as Fig. 2(c) with $L_b - L_r = 15.68$ μm for the resonance at 1557 nm as marked by the arrow in Fig. 2(c). To tune the resonance into the narrowest bandwidth and high extinction ratio, the heaters are set to minimize the output coupling ($\kappa' \sim 0$) and maximize the extinction ratio ($\kappa \sim \alpha$). This is achieved at heating powers of 5.4 mW (heater 1) and 2.0 mW (heater 2), for which the resonance has a bandwidth of ~ 0.1 nm and an extinction ratio higher than 23 dB limited by our setup. This bandwidth can be continuously adjusted with the heating powers. For example, a bandwidth of 0.4 nm is obtained at heating powers of 9.9 and 9.3 mW. At heating powers of 14.4 and 12.0 mW, the bandwidth reaches the maximum of ~ 0.7 nm, which agrees with the expected 0.65 nm [see Fig. 1(c)]. The near-resonance transmission slightly decreases due to the higher coupling level. The minimal bandwidth (0.1 nm) is much larger than the expected 0.01 nm for two reasons: the large attenuation constant induced by fabrication imperfections (mostly sidewall roughness) and the mode conversion loss induced by the very narrow gap (50 nm) in the coupling region [17]. The first issue can be improved with techniques such as pattern preprocessing [16] and resist reflow [18], while the second can be improved with a longer coupling region and a larger gap. The electrical power required for tuning can also be reduced by optimizing the waveguide and heater geometries.

In conclusion, we demonstrate compact microring resonators with a bandwidth continuously tunable from 0.1 to 0.7 nm and an extinction ratio higher than 23 dB. The devices are fabricated on a silicon-

on-insulator substrate and have a footprint less than 0.001 mm². With improved coupling design and fabrication processing, an ultrabroad tuning range from 0.01 nm to a few nanometers can be obtained. Such flexibility and compactness are critical for chip-scale integrated photonic circuits for optical processing and interconnects.

The authors thank the National Science Foundation’s CAREER Grant (No. 0446571) and the Defense Advanced Research Projects Agency’s EPIC program (supervised by Jagdeep Shah and Richard Soref and executed by the Microsystems Technology Office under Contract HR0011-05-C-0027) for supporting this work. This work was performed in part at the Cornell Nano-Scale Science & Technology Facility (a member of the National Nanofabrication Users Network), which is supported by National Science Foundation, its users, and Cornell University and its Industrial Affiliates.

References

1. K. J. Vahala, *Nature* **424**, 839 (2003).
2. M. Pelton, C. Santori, J. Vuckovic, B. Zhang, G. S. Solomon, J. Plant, and Y. Yamamoto, *Phys. Rev. Lett.* **89**, 233602 (2002).
3. A. Srinivasan, S. Murtaza, J. C. Campbell, and B. G. Streetman, *Appl. Phys. Lett.* **66**, 535 (1995).
4. B. E. Little, J. Foresi, G. Steinmeyer, E. R. Thoen, S. T. Chu, H. Haus, E. Ippen, L. C. Kimberling, and W. Greene, *IEEE Photon. Technol. Lett.* **10**, 549 (1998).
5. Q. Xu, B. Schmidt, S. Pradhan, and M. Lipson, *Nature* **435**, 325 (2005).
6. P. Dong, S. F. Preble, and M. Lipson, *Opt. Express* **15**, 9600 (2007).
7. S. Reitzenstein, A. Bazhenov, A. Gorbunov, C. Hofmann, S. Münch, A. Löffler, M. Kamp, J. P. Reithmaier, V. D. Kulakovskii, and A. Forchel, *Appl. Phys. Lett.* **89**, 051107 (2006).
8. A. M. Armani and K. J. Vahala, *Opt. Lett.* **31**, 1896 (2006).
9. B. G. Lee, B. A. Small, K. Bergman, Q. Xu, and M. Lipson, *Opt. Lett.* **31**, 2701 (2006).
10. E. Pawlowski, K. Takiguchi, M. Okuno, K. Sasayama, A. Himeno, K. Okamoto, and Y. Ohmori, *Electron. Lett.* **32**, 113 (1996).
11. P. Koonath, T. Indukuri, and B. Jalali, *J. Lightwave Technol.* **24**, 1796 (2006).
12. J. Yao, D. Leuenberger, M. M. Lee, and M. C. Wu, *IEEE J. Sel. Top. Quantum Electron.* **13**, 202 (2007).
13. L. Zhou and A. W. Poon, *Opt. Express* **15**, 9194 (2007).
14. M. A. Popovic, T. Barwicz, F. Gan, M. S. Dahlem, C. W. Holzwarth, P. T. Rakich, H. I. Smith, E. P. Ippen, and F. X. Kartner, in *Conference on Lasers and Electro-Optics (CLEO)* (Optical Society of America, 2007), paper CPDA2.
15. W. Bogaerts, D. Taillaert, B. Luyssaert, P. Dumon, J. Van Campenhout, P. Bienstman, D. Van Thourhout, R. Baets, V. Wiaux, and S. Beckx, *Opt. Express* **12**, 1583 (2004).
16. J. Niehusmann, A. Vörckel, P. H. Bolivar, T. Wahlbrink, W. Henschel, and H. Kurz, *Opt. Lett.* **29**, 2861 (2004).
17. F. Xia, L. Sekaric, and Y. A. Vlasov, *Opt. Express* **14**, 3872 (2006).
18. M. Borselli, T. J. Johnson, and O. Painter, *Opt. Express* **13**, 1515 (2005).